(5) Yee, A. F.; Smith, S. A. *Macromolecules*, **1981**, *14*, 54.
(6) Hall, C. K.; Helfand, E. *J. Chem. Phys.* **1982**, *77*, 3275.
(7) Viovy, J. L.; Monnerie, L.; Brochon, J. C. *Macromolecules* **1983**, *16*, 1845.
(8) Chiang, J. F.; Wilcox, C. F., Jr.; Bauer, S. H. *J. Am. Chem. Soc.* **1968**, *90*, 3149.
(9) Van Alsenoy, C.; Scarsdale, J. N.; Schafer, L. *J. Comput. Chem.* **1982**, *3*, 53.
(10) Doms, L.; Van den Eden, L.; Geise, H. J.; Van Alsenoy, C. *J. Am. Chem. Soc.* **1983**, *105*, 158. Supplementary material on structure specifications referenced therein also examined.
(11) Szeverenyi, N. M.; Vold, R. R.; Vold, R. L. *Chem. Phys.* **1976**, *18*, 23.
(12) Dill, K.; Allerhand, A. *J. Am. Chem. Soc.* **1979**, *101*, 4376.
(13) Cyvin, S. J. "Molecular Vibrations and Mean Square Amplitudes"; Elsevier: Amsterdam, 1968.
(14) Diehl, P.; Niederberger, W. *J. Magn. Reson.* **1973**, *9*, 495.
(15) Almenningen, A.; Bastiansen, O.; Fernholt, L. *K. Nor. Vidensk. Selsk., Skr.* **1958**, *3*, 8.
(16) Gronski, W.; Murayama, N. *Makromol. Chem.* **1978**, *179*, 1529. Gronski, W. *Makromol. Chem.* **1979**, *180*, 1119.
(17) Schaefer, J.; Stejskal, E. O.; McKay, R. A.; Dixon, W. T. *Macromolecules* **1984**, *17*, 1479.
(18) Garroway, A. N.; Ritchey, W. M.; Moniz, W. B. *Macromolecules* **1982**, *15*, 1051.
(19) Jones, A. A., submitted to *Macromolecules*.

Polymorphic Transformations in Ferroelectric Copolymers of Vinylidene Fluoride Induced by Electron Irradiation

Andrew J. Lovinger

AT&T Bell Laboratories, Murray Hill, New Jersey 07974. *Received August 31, 1984*

ABSTRACT: Electron irradiation of vinylidene fluoride copolymers with tri- or tetrafluoroethylene was found to induce a room-temperature polymorphic transformation of the ferroelectric phase to one that is structurally equivalent to the paraelectric phase normally accessible only above the Curie temperature. This solid-state transformation is irreversible and precedes by far the eventual amorphization that takes place at higher electron doses. Both transformations are extremely sensitive to electron dose, amorphization occurring at ca. 14–20% of the corresponding dose for polyethylene, and polymorphic transformation at ca. 4–9% of the same dose. This polymorphic transformation is highly unusual in that it does not yield an intermolecularly defective lattice as do electron-induced transformations in other polymers; on the contrary, evidence from electron diffraction and dark-field electron microscopy shows that the resulting paraelectric-like phase exhibits significantly higher lattice perfection than the original ferroelectric phase. PVF_2 homopolymer (β-phase) does not undergo such an electron-induced transformation prior to amorphization. An explanation for the susceptibility of the copolymers, but not of the homopolymer, to polymorphic transformation is offered on the basis of structural differences between the two.

Introduction

Ferroelectric-to-paraelectric phase transformations in random copolymers of vinylidene fluoride (VF_2) and trifluoroethylene (F_3E) have been demonstrated in the last few years.[1-4] The molecular conformation of these copolymers in their ferroelectric phase is the same as in β-PVF_2, i.e., essentially all *trans* (TT); above the Curie temperature, this conformation changes to a disordered sequence of TG, T$\bar{G}$, and TT units as a result of the introduction of *gauche* bonds.[3,4] In both ferroelectric and paraelectric phases, the copolymer chains are packed on a lattice that is very close to hexagonal.[3,4] Similar transitions have recently been found also in a copolymer of vinylidene fluoride with tetrafluoroethylene (F_4E),[5,6] proving that this Curie behavior is not a result of any particular comonomer, but is an inherent property of the homopolymer, poly(vinylidene fluoride) (PVF_2); the latter copolymer (VF_2/F_4E) is, in fact, equivalent to PVF_2 having an increased content of head-to-head (i.e., CF_2–CF_2) defects.[7] On the other hand, PVF_2 homopolymer does not show a clear ferroelectric-to-paraelectric solid-state transformation upon heating. On the basis of the variation of the Curie temperature with VF_2 content in VF_2/F_3E copolymers, it was concluded[3] that for β-PVF_2 such a transition should be centered slightly above the melting point; the role of melting in aborting an ongoing ferroelectric-to-paraelectric transformation was clearly demonstrated in that study[3] for a 78/22 mol % VF_2/F_3E copolymer. In addition, indications of the earliest stages of such a transition have been recently reported for β-PVF_2 at temperatures just below the melting point.[4]

While such ferroelectric-to-paraelectric phase transformations are only a very rare and recently discovered phenomenon among polymers,[8] other crystallographic transformations are, of course, common and well-known. Within that category lie electron-induced transformations which generally lead to loss of crystallinity as a result of cross-linking or chain scission, but which may also include intermediate crystallographic phase changes.[9] The most widely studied polymer in this regard is polyethylene, which undergoes an orthorhombic-to-hexagonal phase transformation en route to amorphization when irradiated by electrons.[10-13] This transformation is evidenced by the following sequential changes that occur in the electron-diffraction pattern of single crystals of orthorhombic polyethylene during observations in the electron microscope: disappearance of the outer *hk*0 reflections, broadening of the inner *hk*0 reflections, increase in the (200) spacing to a value characteristic of the (110) spacing (thus leading to hexagonal symmetry), and, finally, fading of the remaining six reflections and their replacement by an amorphous halo. These manifestations are a direct consequence of the chemical and structural changes that result in cross-linking due to formation of free radicals by the high-energy electrons. Specifically, cross-linking causes at first crystalline distortions (with consequent loss of the outer *hk*0 reflections and broadening of the inner ones), followed by continuous expansion of the *a* axis of the unit cell (to the point of attainment of hexagonal symmetry), and eventually full amorphization. Similar phenomena have also been observed in other polymers, e.g., in even–even polyamides, where the separation between the (100) and (010/110) reflections was found to decrease with electron bombardment as these reflections were simultaneously becoming broader and more diffuse.[14]

These two areas—electron-induced phase changes and ferroelectric-to-paraelectric transitions—have been brought together in this study. An irreversible transformation of

0024-9297/85/2218-0910$01.50/0

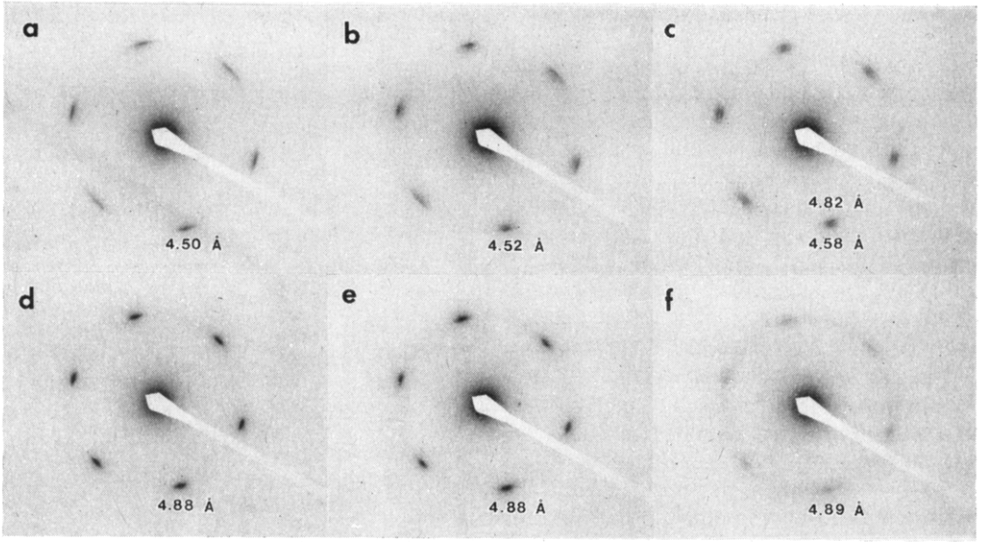

Figure 1. Consecutive room-temperature electron-diffraction patterns from a single crystal of a 73/27 mol % VF_2/F_3E copolymer grown from the melt at 135 °C and examined normal to the electron beam: (a) initial exposure, (b) after 3 C/m^2, (c) after 4 C/m^2, (d) after 6 C/m^2, (e) after 9 C/m^2, and (f) after 14 C/m^2.

the ferroelectric lattice in VF_2/F_3E and VF_2/F_4E copolymers is reported here that takes place at room temperature during electron irradiation of thin films; this solid-state transformation leads to an intermediate lattice (that is structurally analogous to the paraelectric) well before the onset of amorphization. This transformation is also remarkable insofar as the intermediate paraelectric lattice is not highly damaged (as described above for its hexagonal counterpart in polyethylene), but appears, in fact, *less* defective intermolecularly than the initial ferroelectric lattice. The dose dependence and morphological changes accompanying this solid-state transformation are also examined, as is the behavior of PVF_2 homopolymer under the same conditions. Finally, an interpretation of the findings discovered here is offered at the end of the paper.

Experimental Section

The materials used here were poly(vinylidene fluoride) homopolymer (KF-1100 manufactured by Kureha Chemical Industry Co., Ltd.), a series of vinylidene fluoride/trifluoroethylene copolymers having 52, 65, 73, and 78 mol % VF_2, respectively (kindly donated by Daikin Kogyo Co., Ltd.), and an 81/19 mol % vinylidene fluoride/tetrafluoroethylene copolymer (Kynar 7200 produced on an experimental basis by Pennwalt Corp.).

Samples of these were cast on the atomically clean surfaces of freshly cleaved mica in the form of ultrathin films (10–20 nm thick) suitable for electron microscopy and diffraction, by dissolution in dimethylformamide, followed by evaporation of the solvent and drying in a vacuum oven for 1 day at 120 °C. The films were then melted and recrystallized isothermally at various temperatures in an atmosphere of dried nitrogen. After predetermined periods of time, the samples were cooled to room temperature and then transferred to a vacuum evaporator for oblique shadowing with Pt/C (to increase electron contrast) and backing with amorphous carbon (to increase their strength). The films were finally floated off their substrates in distilled water and deposited on copper grids for electron-microscopic examination at 100 keV.

In order to reduce to the extent possible any instrumental contributions to the broadening of reflections, as well as to minimize the rate of radiation damage to the specimens, a combination of low beam current, small second-condenser aperture, and extremely small beam divergence (in the 10^{-6}-rad range) was used. To allow rapid photographic recording of essentially instantaneous time frames of the radiation-induced crystallographic changes, a very sensitive, low-background emulsion (CEA Reflex 15, Strengaes, Sweden) was used, and the electron beam was turned off at times other than the actual recording. Under such conditions, photographic exposures as short as 2 s could be made with a radiation lifetime exceeding 100 s. Electron doses were measured by using a Faraday-cup specimen holder that had been connected to a picoammeter. Dark-field electron micrographs could only marginally be recorded by using a single diffracted beam in the conventional transmission mode, so that a simultaneous multiple-beam technique employing all inner reflections was utilized in the scanning-transmission mode.[15]

Results

The copolymers of VF_2 with F_3E or F_4E studied here lose their crystalline diffraction features under irradiation in the electron microscope by a cross-linking mechanism, as does polyethylene. However, well before that occurs, a crystallographic transformation takes place that is illustrated below for single crystals of a 73/27 mol % VF_2/F_3E copolymer grown at high temperature. The diffraction pattern of Figure 1a is the first of a sequence photographed during irradiation of one such single crystal with the beam normal to the film plane. This figure reproduces only the innermost reflections, which are of the *hk*0 type, and exhibits the metrically hexagonal symmetry expected of the intermolecular packing of the chain stems in their ferroelectric phase.[3] Their spacing is somewhat larger than determined by X-ray diffraction (4.40–4.46 Å) because of a slight expansion of the unit cell during electron diffraction; this is a common phenomenon that has also been observed during electron diffraction of single crystals of PVF_2 homopolymer,[16] and is not inherent to the transformation described in this paper. Evidence for the *inter*molecular aspects of this transformation is provided in Figure 1b–d, which represent successive diffraction patterns from the same crystal: the reflections at 4.50 Å are seen to decrease in intensity, while new reflections appear at a higher spacing and eventually replace the original ones. Specific attention should be paid to the following features of this solid-state transformation that render it radically different from the common electron-induced changes seen in polyethylene and other polymers:[10–14] (1) The new lattice does not grow through continuous expansion of the original one; there is only very limited expansion of both lattices during irradiation, while it is clear that the new lattice grows *at the expense* of the original one and that *both* coexist at intermediate electron doses (Figure 1c). (2) The new lattice is not a damaged and defective version of the original one; no diffuseness or broadening of reflections is observed, while the higher orders of reflections are

preserved through the stage depicted in Figure 1d. On the contrary, Figure 1a–d indicates that there is a quite surprising *increase* in apparent lattice perfection accompanying this solid-state transformation. Evidence for this is found in the much higher intensity of reflections of the new lattice (Figure 1d) compared to the original one (Figure 1a), and in their decreased arcing and breadth (although the latter may not be readily evident in Figure 1d due to the response of the photographic emulsion to the greatly increased intensity). It should be noted by comparing, e.g., Figures 1a, and c, that reflection arcing is reduced even for the original ferroelectric lattice during irradiation, implying that lateral misorientations are being removed.

Following this polymorphic transformation, further changes in the electron-diffraction patterns of such copolymers are seen in Figure 1d,e. At this stage, the electron-induced effects are now typical of what is exhibited by most other polymers, i.e., ongoing amorphization due to cross-linking, as witnessed by the broadening and eventual disappearance of crystallographic reflections.

The obvious question at this point concerns the identification of the new lattice that is formed during electron irradiation. Its major d spacing at 4.88 Å is characteristic of the paraelectric lattice of this copolymer, as determined by X-ray diffraction above the Curie temperature[3] (keeping in mind once again the slight expansion associated with electron examination). However, while the *inter*molecular spacing may suggest the paraelectric structure, we must also examine the *intra*molecular evidence in order to reach a more definitive conclusion. In order to bring the $00l$ reflections to the Ewald sphere, the samples must be tilted by 90° from their original position (normal to the beam), which is, of course, impossible in the electron microscope: the largest tilt angle attainable is 60°. We found that, at this angle, some areas of the polymer film yield $00l$ reflections, presumably because our ultrathin samples were buckled in that location. The response of one such area to electron irradiation is reproduced in Figure 2. There, the all-*trans* conformation of the original ferroelectric lattice is evident in the (001) and (201,111) reflections at 2.57 and 2.23 Å, respectively, in Figure 2a (these Miller indices are referred to orthohexagonal coordinates for consistency with β-PVF_2). We should also notice that, in agreement with other polymers,[9] the intramolecular d spacing is not expanded in the electron microscope as are its intermolecular counterparts. Upon initial irradiation, Figure 2b shows that, simultaneously with the replacement of the intermolecular ferroelectric reflection at 4.53 Å by that of the new phase (at 4.92 Å), the intramolecularly associated reflections of Figure 2a are also replaced by a weak, broad, and diffuse reflection at 2.29 Å. We have previously found the same changes when these copolymers were heated above their Curie temperatures;[3] the spacing, breadth, and diffuseness of the reflection at 2.29 Å were the same as observed here and were attributed to the intramolecular repeat of a disordered conformation consisting of random TG, T$\bar{G}$, and TT sequences.[3] Figure 2c indicates the incipient amorphization accompanying further electron irradiation of this copolymer.

Because the intramolecular reflection at 2.29 Å in Figure 2b is so weak and broad that it may be confused with an amorphous halo, we have grown crystals of the same copolymer in such an orientation that the $00l$ reflections would be tangent to the Ewald sphere without any specimen tilting, thus allowing maximization of their intensity. Lamellae of this copolymer were grown essentially on edge (i.e., perpendicular to the thin-film surface) by epitaxial

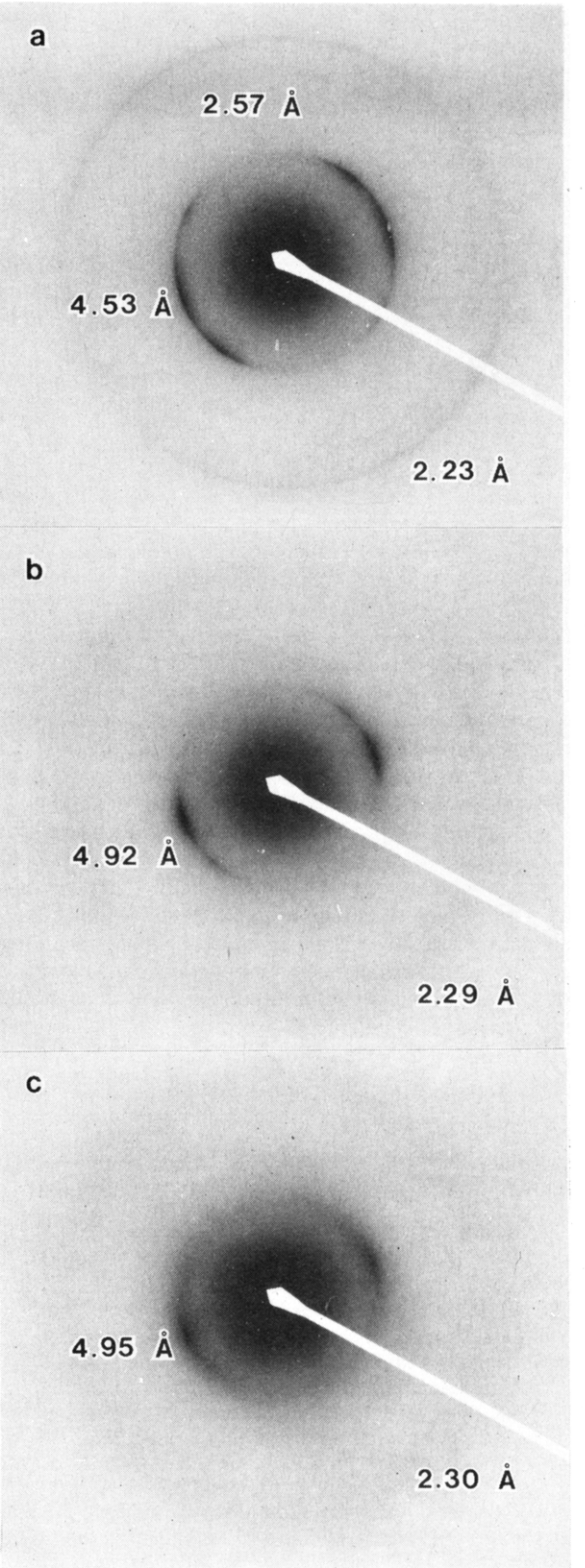

Figure 2. Consecutive room-temperature electron-diffraction patterns from crystals of a 73/27 mol % VF_2/F_3E copolymer grown from the melt at 135 °C and tilted by 60° with respect to the electron beam: (a) initial exposure, (b) after 9 C/m^2, and (c) after 16 C/m^2.

crystallization on the freshly cleaved (001) surface of potassium bromide. The well-known cross-hatched morphology of polymeric lamellae grown on alkali halides parallel to the [110] and [1$\bar{1}$0] directions[17] is clearly seen in this case (Figure 3d). The diffraction pattern of such an assembly of crystals is seen in Figure 3a–c at increasing stages of electron irradiation. The initial pattern prior to

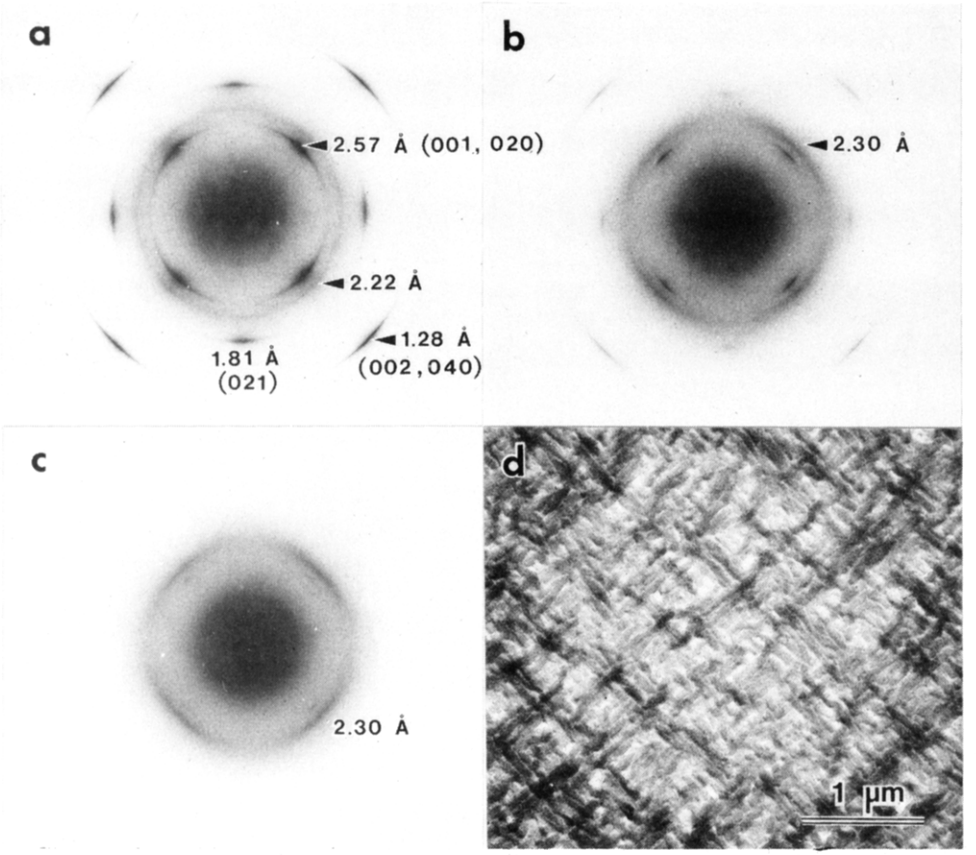

Figure 3. (a–c) Consecutive room-temperature electron-diffraction patterns from crystals of a 73/27 mol % VF_2/F_3E copolymer grown epitaxially from the melt onto KBr. (d) Bright-field electron micrograph of the crystals producing the accompanying diffraction patterns.

any substantial effect of the electron beam (Figure 3a) shows that the reflections belong to a $0kl$ reciprocal net of the ferroelectric lattice (as before, these reflections are referred to orthohexagonal axes). This implies that nucleation of the polymer took place with the (200) [equivalent to {110}] planes in contact with the substrate and explains the absence of these strongest intermolecular reflections at 4.50–4.53 Å (previously observed in Figures 1 and 2). Because the (020) [equivalent to {310}] d spacing for this copolymer is coincidentally almost exactly the same as that of the (001), and because of the double orientation at 90° due to epitaxy, the (001) and (020) reflections are overlapped in the diffraction pattern of the ferroelectric phase (Figure 3a).

As the sample is irradiated, the accompanying changes in its electron-diffraction pattern are seen in Figure 3b,c. Hence, the broad and diffuse reflection at 2.30 Å that is expected from the conformation of the paraelectric phase is clearly observable. From the streaked appearance of this reflection we infer that the molecular chains are partly decorrelated along c, as would be expected by the substantially random introduction of G and $\bar{G}$ bonds during the transformation. It is also seen in these figures that the reflections attributable to the intermolecular packing decay more rapidly than this intramolecular reflection at 2.30 Å; this is in agreement with the behavior of other polymers[9,11] and is explained by the highly disruptive effects of cross-linking on the intermolecular lattice. In summary, then, our electron-diffraction results using both inter- and intramolecular evidence show that a solid-state transformation of the ferroelectric lattice to one that is structurally identifiable as the paraelectric takes place during the early stages of electron irradiation. The same behavior applies to all the VF_2/F_3E and VF_2/F_4E copolymers studied in this work.

Table I
Doses Required for Crystallographic Effects of Electron Irradiation in Various Polymers[a]

	dose, C/m^2	
polymer[b]	ferroelectric-to-paraelectric transformn	destructn of crystallinity
polyethylene (linear)		102 ● 4
poly(vinylidene fluoride), α-phase		31 ● 2
poly(vinylidene fluoride), β-phase		39 ± 2
poly(vinylidene fluoride), γ-phase		36 ± 2
vinylidene fluoride/trifluoroethylene copolymer		
52/48 mol %	4 ± 1	14 ± 1
65/35 mol %	4 ± 1	18 ± 2
73/27 mol %	6 ± 1	18 ± 1
78/22 mol %	7 ± 1	17 ± 1
poly(trifluoroethylene)		14 ± 1
vinylidene fluoride/tetrafluoroethylene copolymer: 81/19 mol %	9 ± 1	21 ± 1

[a] Mean ± sample standard deviation for 7–10 measurements. [b] PE single crystals were grown from dilute solution in p-xylene; α-PVF_2 single crystals were obtained from a dilute solution of monochlorobenzene/dimethylformamide 90/10; all other samples consisted of single crystals grown from the melt in ultrathin films at high temperatures, except for β-PVF_2, which was obtained in oriented form by uniaxial deformation of α-PVF_2 at room temperature.

A most noteworthy aspect of this electron-induced solid-state transformation is its exceptionally high sensitivity to electron dose. This is summarized in Table I, where doses (average ± standard deviation) are given for a number of polymers. Polyethylene is used as a standard of reference, since most of the studies on electron-induced

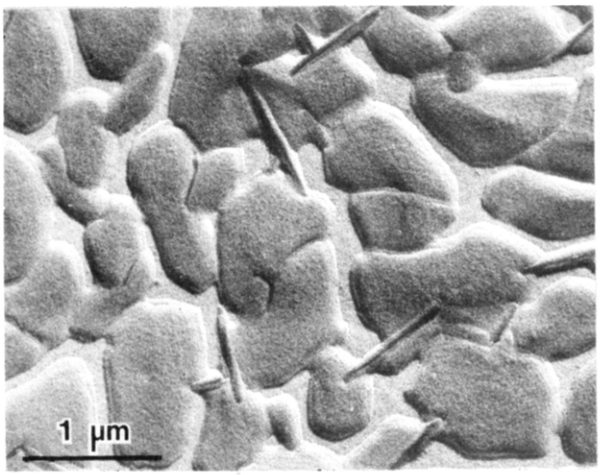

Figure 4. Electron-microscopic appearance (bright-field) of typical single crystals of a 65/35 mol % VF_2/F_3E copolymer grown from the melt in thin films at 135 °C.

crystallographic changes have been conducted on this material; vinylidene fluoride and trifluoroethylene homopolymers are also included for comparison. It is seen in this table that PVF_2 becomes amorphous under the electron beam at about one-third of the corresponding dose for polyethylene, while PF_3E and the copolymers are even more electron sensitive, requiring only one-seventh to one-fifth of that dose. What is remarkable is the very much smaller dose needed to elicit the ferroelectric-to-paraelectric transformation in these copolymers, which is seen in Table I to be 4–9 C/m^2 (this is defined as the dose required to change the diffraction pattern so as to bring the paraelectric-phase reflections to maximal sharpness and intensity, as in Figure 1d). Therefore, this polymorphic transformation is apparently one of the most electron-sensitive phenomena observed to date.

At this point, let us examine the morphology of the single crystals that led to the diffraction evidence for this solid-state transformation. A bright-field electron micrograph of a 65/35 mol % VF_2/F_3E thin film crystallized at 135 °C is seen in Figure 4. With the exception of a few rodlike entities (which are simply lamellae nucleated on the substrate and thus grown on edge), the sample consists of platelet-like single crystals seen flat-on and having totally irregular boundaries. The most striking feature of these crystals is precisely their irregular boundaries, since the macroscopic regularity implicit in a single crystal is almost always associated with sharp and straight crystallographic growth faceting. The lack of such regular faceting is attributed to the irregular molecular structure of these crystals: not only are they random copolymers, but their F_3E component is also added in an atactic manner with a significant amount of regioirregularity. In addition, the high temperatures required for single-crystal growth lie above that of the paraelectric-to-ferroelectric transition, so that the crystals of Figure 4 were originally grown with the disordered molecular conformation of the paraelectric phase. These crystals are in fact morphologically indistinguishable from those of poly(trifluoroethylene) homopolymer, for which we have used the same rationale to explain their lack of expected crystallographic faceting.[19] At lower crystallization temperatures, lamellar aggregates and immature spherulites are obtained instead of the single crystals studied so far. However, these also undergo the same ferroelectric-to-paraelectric transformation under electron bombardment, as seen in Figure 5. Full diffraction rings are now obtained since the area contributing to the recorded pattern contains the multi-

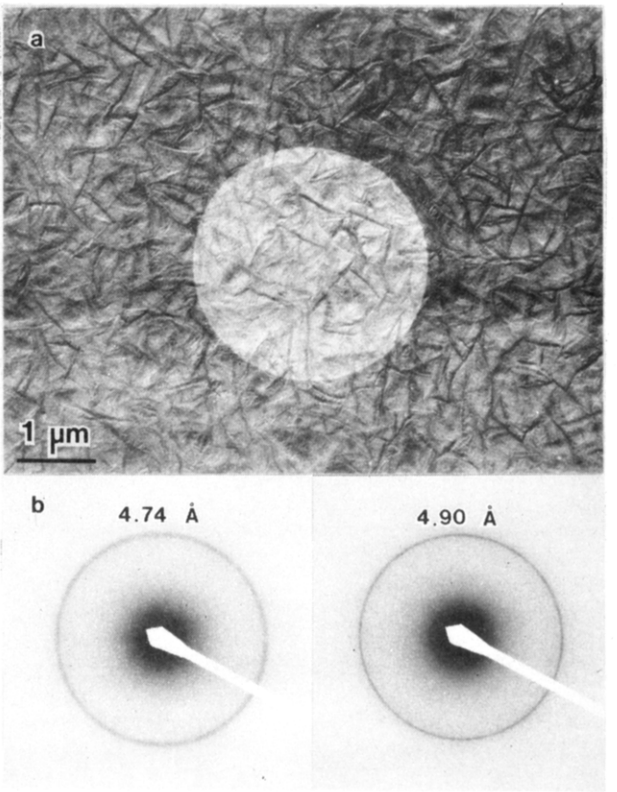

Figure 5. (a) Electron-microscopic appearance (bright-field) of a thin-film sample of a 52/48 mol % VF_2/F_3E copolymer quenched from the melt to room temperature. (b) Electron-diffraction patterns from the circled area of part a before and after the electron-induced solid-state transformation.

tude of lamellae delineated in the center of the bright-field electron micrograph of this figure. The ring at 4.90 Å corresponding to the intermolecular spacing of the paraelectric phase is clearly seen to be stronger and sharper than that of the original ferroelectric phase, as was also the case for the equivalent reflections in single crystals (Figure 1a,d).

This increased strength and perfection of the paraelectric-phase reflections is most surprising, since the molecular effects of the electron beam should decrease, rather than increase, the crystalline order; such disordering has been clearly documented for the orthorhombic → hexagonal electron-induced transformation in polyethylene.[10-12] In an effort to understand the origin of this phenomenon, we examined the changes in the dark-field image from the same area of the sample with continued electron irradiation. Because of the extremely short life of each stage of the transformation, annular dark-field scanning-transmission electron microscopy was used, with all beams centered at 4.50–4.90 Å contributing to the recorded image. A series of such dark-field micrographs is seen in Figure 6a–e; the corresponding bright-field image is depicted in Figure 6f and shows the diffracting area to consist of a part of a large single crystal that includes some lamellar overgrowths. The initial dark-field micrograph (Figure 6a) (equivalent to the diffraction pattern of Figure 1a) shows that the ferroelectric-phase reflections arise from only a limited fraction of the crystal, and specifically from small, isolated crystallites that do not exceed 100 nm in mean dimension. Under continued irradiation (Figure 6b, corresponding approximately to Figure 1c) more of the sample appears to diffract, and when the paraelectric lattice is fully adopted (Figure 6c, approximately equivalent to Figure 1d), large areas of the sample are diffracting coherently. Diffraction contrast is diminished upon further electron

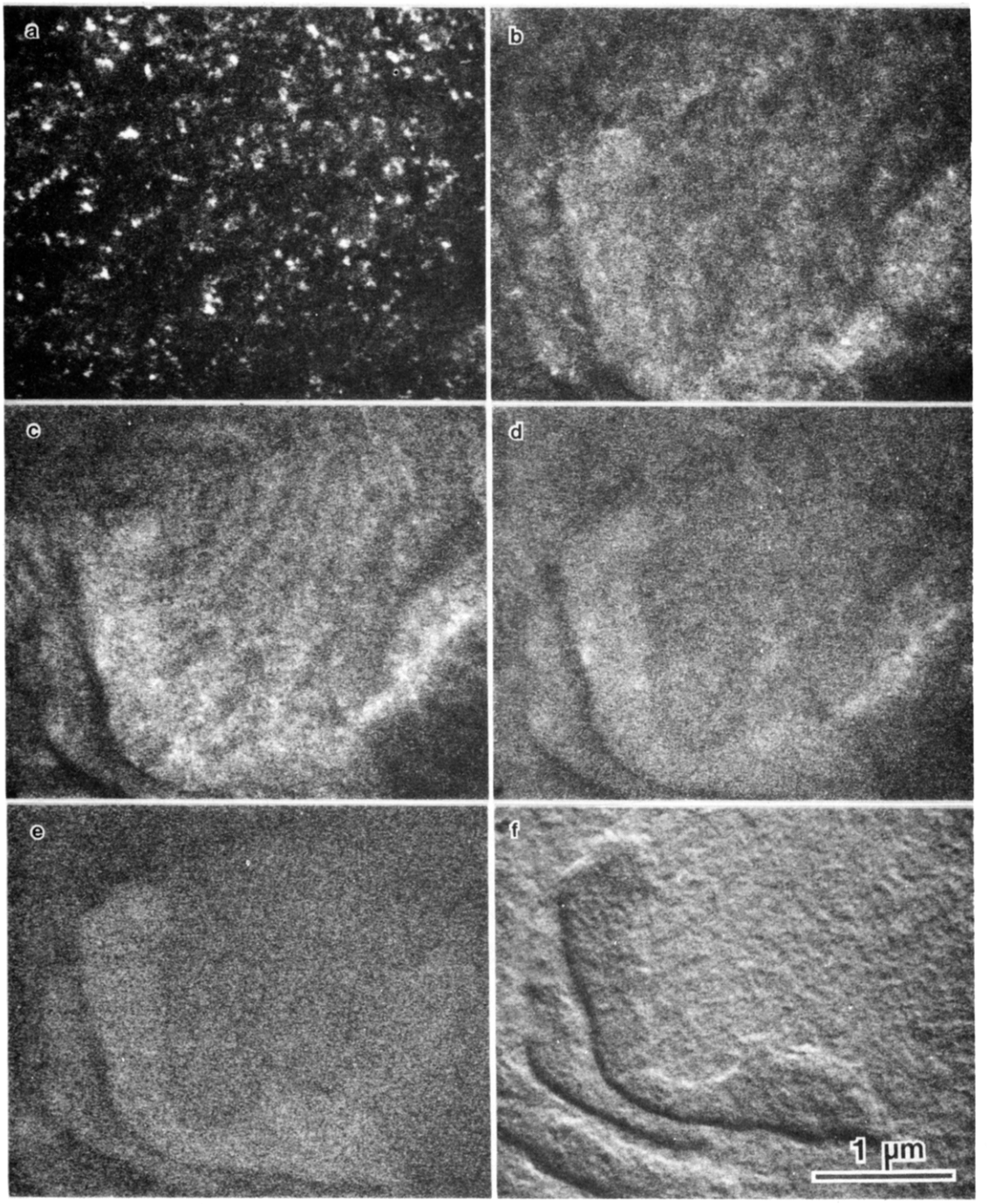

Figure 6. (a–e) Consecutive multiple-beam dark-field electron micrographs from a 73/27 mol % VF_2/F_3E copolymer crystallized at 130 °C and showing the regions diffracting at each state of the solid-state transformation. (f) The same area of the specimen recorded in bright field after completion of the dark-field sequence.

exposure (Figure 6d) and eventually lost (Figure 6e) as the irradiated area has become fully cross-linked. A general "brightening" of the imaged area is common in dark-field electron microscopy due to the amorphous scattering that contributes increasingly during irradiation. However, this cannot lie at the root of the considerably increased luminosity of Figure 6c, because (a) the coherently diffracting regions stand out clearly in that area, (b) the contribution of the fully amorphous specimen can be judged from Figure 6e, and (c) a comparison of the diffracted-beam intensities in Figure 1a,d demonstrates convincingly the highly increased crystallographic contribution to the dark-field intensity of Figure 6c. We are therefore brought to the conclusion that, contrary to expectations based on the behavior of other polymers, this electron-induced solid-state transformation is indeed accompanied by an increase in the overall crystalline order. This may be readily explained if we recall the thermal history of our copolymer samples: Although the initial reflections observed during electron diffraction arise from the ferroelectric phase, this does not imply that the crystals were originally grown in that phase. On the contrary, the high temperatures required for single-crystal growth cause those crystals to grow originally with the paraelectric lattice and to transform to its ferroelectric counterpart only upon subsequent cooling to room temperature. This solid-state transformation entails a significant contraction of the intermolecular lattice (e.g., the reduction in area for the 73/27 mol % VF_2/F_3E copolymer is ca. 15%). It is, therefore, expected to cause the original crystals to break up into smaller crystallites. In addition, the resulting stresses on these crystallites may bend some of them away

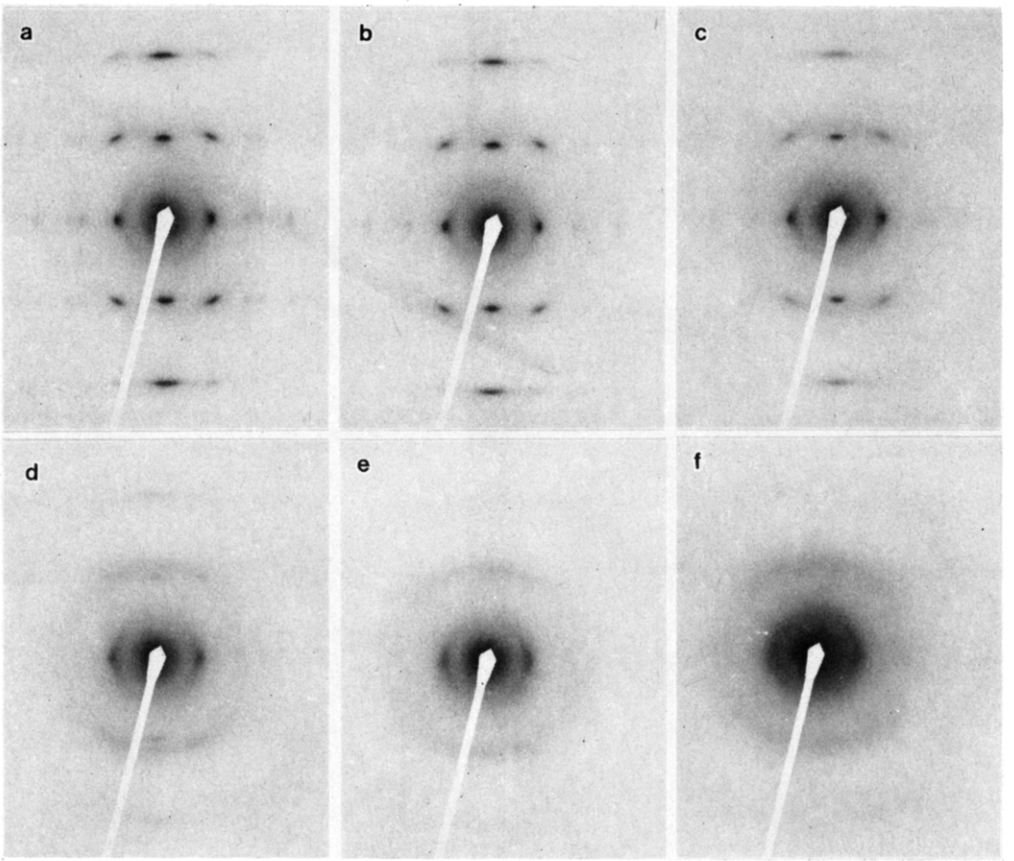

Figure 7. Consecutive room-temperature electron-diffraction patterns from uniaxially oriented β-PVF_2 (fiber axis vertical): (a) initial exposure, (b) after 9 C/m^2, (c) after 20 C/m^2, (d) after 25 C/m^2, (e) after 32 C/m^2, and (f) after 38 C/m^2.

from the reflecting position, yielding the appearance of Figure 6a. On the other hand, the expansion back to a paraelectric lattice during electron irradiation should relieve those stresses and substantially restore the original macroscopic coherence within each crystal, leading to the dark-field image of Figure 6c and to the observed increase in diffracted intensity.

Discussion

Our results so far have shown that an irreversible transformation from the ferroelectric phase to one that is structurally equivalent to the paraelectric can be induced at room temperature in copolymers of vinylidene fluoride with tri- or tetrafluoroethylene by exposing them to electron bombardment. This raises the intriguing possibility of effecting a similar transformation in PVF_2 *homopolymer* (β-phase), where the traditional, thermally induced, Curie transition is centered above the melting point and has therefore been inaccessible to complete characterization. Such an electron-initiated transformation should be *a priori* plausible, because the chain conformation and packing in the ferroelectric phases of both β-PVF_2 and the aforementioned copolymers are essentially the same. Since β-PVF_2 cannot be obtained in the form of single crystals through direct crystallization, it was obtained instead by uniaxial deformation of very thin α-PVF_2 films at room temperature. Electron-diffraction patterns of one such film during successive stages of irradiation are seen in Figure 7. The crystallographic changes observable in this figure are consistent with an ongoing amorphization due to cross-linking, as seen by the early loss of the higher-order reflections, the gradual introduction of broadening and diffuseness to the remaining ones, and their eventual replacement by amorphous haloes. However, in sharp contrast to the copolymers, there is no evidence of any polymorphic transformation preceding amorphization.

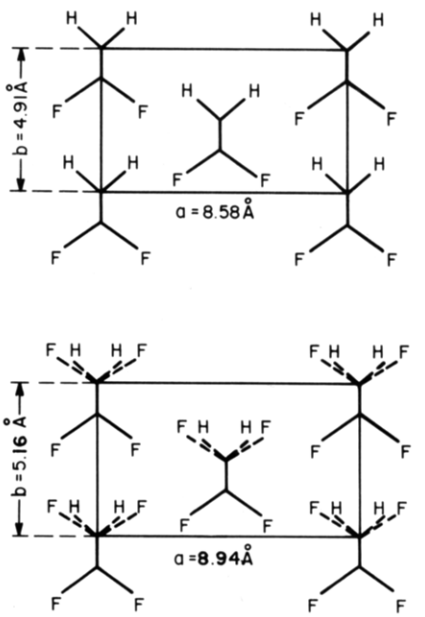

Figure 8. Unit cell of β-PVF_2 (top) and of the ferroelectric phase of a 73/27 mol % VF_2/F_3E copolymer (bottom), projected along the molecular axis.

There are, consequently, two major questions that must now be addressed: (1) why do the copolymers undergo this intermediate crystallographic transformation from their ferroelectric lattice during electron bombardment, and (2) why does the homopolymer itself *not* undergo the same transformation. An explanation is offered here for both questions on the basis of the structural characteristics of the ferroelectric phases of β-PVF_2 and its copolymers. The *ab* cell base of β-PVF_2 and of one representative composition of these copolymers (73/27 mol % VF_2/F_3E) is

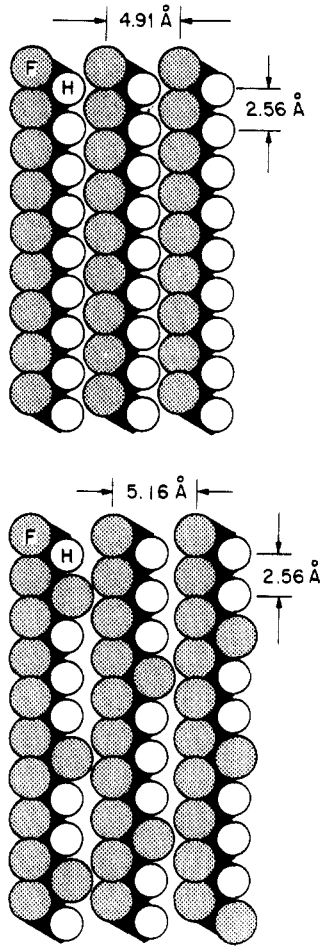

Figure 9. Schematic models of chain packing in the *bc* plane of β-PVF_2 (top) and of the ferroelectric phase of a 73/27 mol % copolymer (bottom).

depicted schematically in Figure 8. In both cases the molecular conformation is the same (essentially *trans*-planar, with small statistical deviations away from that plane); the intermolecular lattice structure, chain packing, and dipolar alignment are also the same. The major structure difference between the homopolymer and its copolymers involves the spacing of their intermolecular lattice. As is seen in Figure 8, both the *a* and the *b* axes of the unit cell are significantly expanded in the copolymers because of the presence of the additional fluorine atoms in tri- and tetrafluoroethylene (since trifluoroethylene is added stereoirregularly,[18] there is an equal distribution of fluorine atoms on both sides of the planar zigzag in VF_2/F_3E copolymers).

As a result of this lattice expansion, the VF_2 units in the copolymers will *not* be in close contact, contrary to the situation in β-PVF_2 homopolymer. This is illustrated schematically in Figure 9 with the aid of *a*-axis projections of molecular space-filling models. In β-PVF_2, the 4.91-Å spacing is determined by the closest possible chain packing in the *b* direction. Since this is also the dipolar direction, the chains are held together by strong attractive forces, so that any intramolecular rotation will be sterically hindered and energetically unfavorable. In the copolymers, on the other hand, the closest contact of the chains along β will take place at the randomly located CFH or CF_2 units; the vinylidene fluoride units are well separated and should therefore be able to rotate more freely toward the *gauche* position. One of the earliest results of electron irradiation in polymers is expansion of the effective cross-sectional area of the chains due to the introduction of internal chemical and structural defects. Such expansion is suppressed to a large degree in β-PVF_2 because of the close contact of the chains throughout their lengths (other, perhaps, than in the regions of head-to-head/tail-to-tail defects), which provides steric conflicts and promotes intermolecular cross-linking. Chains of the copolymers are more free to expand transversely by incorporation of structural defects and, in so doing, to attain the localized energy minimum corresponding to the paraelectric-lattice spacing. They are also more susceptible to transformation since they originate from the macroscopically defective ferroelectric lattice.

A final point concerns the relationship between the paraelectric-like phase obtained here by electron irradiation and the true paraelectric phase arising at high temperatures. First of all, it should be made clear that the effects of the electron beam are overwhelmingly chemical and only negligibly thermal:[9] the temperature rise under our experimental conditions can be calculated[9] to be less than 1 °C and use of eicosane under the same experimental conditions confirmed that its melting temperature (37 °C) was not exceeded. Therefore, the paraelectric phase obtained by electron bombardment does not result from local overheating beyond the Curie temperature. From the structural point of view, the two paraelectric phases are clearly similar, albeit not identical: while the electron-irradiated phase has similar intra- and intermolecular spacings as its thermally induced counterpart, it is also certain to contain a significant number of chemical defects, including ionic groups, free radicals, double bonds, and intramolecular and intermolecular linkages (which render this an irreversible solid-state transformation). The similarities have at their root the disordering introduced, respectively, by the effects of electron irradiation vs. thermal activation. Since any departure from an all-*trans* conformation would tend to favor other low-energy rotational isomers, random introduction of *gauche* and *gauche*$^-$ bonds should occur both under the electron beam and above the Curie temperature, thus leading naturally to the disordered sequences of TG, T$\bar{\text{G}}$, and TT groups that characterize the paraelectric conformation. The transversely expanded chains resulting from either of these processes will then tend to be packed in expanded lattices, as shown experimentally. Other than these structural similarities and differences, nothing can be said at this stage about the relationships between the thermally and the electron-induced paraelectric phases, including, for example, piezoelectric and dielectric characteristics. It is expected that the conformational and packing changes resulting from electron irradiation should lead to loss of piezo- and pyroelectricity, although this could not be tested in our samples since they are extremely thin and contain only small, discrete areas that had been subjected to the high-energy beam. γ-Irradiation of macroscopic specimens should provide the answers to these and other related questions.

Conclusions

Electron irradiation of copolymers of vinylidene fluoride with trifluoroethylene or tetrafluoroethylene causes a solid-state transformation at very low doses (4–9 C/m^2); continued irradiation leads to an amorphous, cross-linked structure at doses of 14–21 C/m^2 that are still far lower than those for other typical polymers (e.g, ca. 102 C/m^2 for linear polyethylene). Both intra- and intermolecular evidence from electron-diffraction analysis shows that the intermediate phase arising during irradiation is structurally analogous to the paraelectric phase normally obtained above the Curie temperature. The ferroelectric β-phase

of PVF_2 homopolymer does not undergo a similar solid-state transformation during electron irradiation, but degrades directly to an amorphous structure. This discrepancy in behavior between homopolymer and copolymers is correlated with molecular and crystallographic differences that allow greater freedom of intramolecular bond rotations in the latter. Single crystals of these copolymers grown at high temperatures lack distinct growth facets, as was also found earlier for poly(trifluoroethylene); this morphological irregularity is ascribed in both cases to chemical, configurational, and conformational disorder. Dark-field electron microscopy at room temperature shows the copolymer lamellae to consist of small, fragmented crystallites, which, however, combine into larger, coherently scattering areas during electron irradiation. This fragmentation is attributed to lattice changes accompanying the paraelectric-to-ferroelectric transformation during cooling of the crystals to room temperature, while the subsequent electron-induced healing is ascribed to the return to a structural analogue of the original paraelectric lattice.

Registry No. (VF_2)-(F_3E) (copolymer), 28960-88-5; (VF_2)-(F_4E) (copolymer), 25684-76-8.

References and Notes

(1) Furukawa, T.; Johnson, G. E.; Bair, H. E.; Tajitsu, Y.; Chiba, A.; Fukada, E. *Ferroelectrics* **1981**, *32*, 61.
(2) Higashihata, Y.; Sako, J.; Yagi, T. *Ferroelectrics* **1981**, *32*, 85.
(3) Lovinger, A. J.; Furukawa, T.; Davis, G. T.; Broadhurst, M. G. *Polymer* **1983**, *24*, 1225, 1233.
(4) Tashiro, K.; Takano, K.; Kobayashi, M.; Chatani, Y.; Tadokoro, H. *Polymer* **1983**, *24*, 199.
(5) Lovinger, A. J. *Macromolecules* **1983**, *16*, 1529.
(6) Lovinger, A. J.; Johnson, G. E.; Bair, H. E.; Anderson, E. W. *J. Appl. Phys.* **1984**, *56*, 2412.
(7) Lando, J. B.; Doll, W. W. *J. Macromol. Sci., Phys.* **1968**, *B2*, 205.
(8) For a general review, see: Lovinger, A. J. *Science* **1983**, *220*, 1115 and references therein.
(9) Grubb, D. T. *J. Mater. Sci.* **1974**, *9*, 1715.
(10) Orth, H.; Fischer, E. W. *Makromol. Chem.* **1965**, *88*, 188.
(11) Kobayashi, K.; Sakaoku, K. *Lab. Invest.* **1965**, *14*, 1097.
(12) Kiho, H.; Ingram, P. *Makromol. Chem.* **1968**, *118*, 45.
(13) Thomas, E. L.; Sass, S. L. *Makromol. Chem.* **1973**, *164*, 333.
(14) Keller, A. *J. Polym. Sci.* **1959**, *36*, 361.
(15) Chacko, V. P.; Adams, W. W.; Thomas, E. L. *J. Mater. Sci.* **1983**, *18*, 1999.
(16) Sakaoku, K.; Peterlin, A. *J. Macromol. Sci., Phys.* **1967**, *B1*, 401.
(17) Willems, *J. Discuss. Faraday Soc.* **1958**, *25*, 111.
(18) Yagi, T.; Tatemoto, T. *Polym. J.* **1979**, *11*, 429.
(19) Lovinger, A. J.; Cais, R. E. *Macromolecules* **1984**, *17*, 1939.

Electron Paramagnetic Resonance Investigation of Orientation Produced by Mechanical Processing in the Fillers of Polymer Composites

Antal Rockenbauer,* László Jókay, Béla Pukánszky, and Ferenc Tüdös

Central Research Institute for Chemistry, Hungarian Academy of Sciences, H-1525 Budapest, Hungary.

Received June 18, 1984

ABSTRACT: Electron paramagnetic resonance spectroscopy has been applied in order to study the orientation effects of mechanical deformation of the calcium carbonate fillers of polymer composites. The anisotropic signals of Mn^{2+} ions substituting Ca^{2+} ions and electron defect centers in calcium carbonate served as spin probes in these studies. The morphology of the calcium carbonate crystallites was found to play a dominant role in the effectivity of ordering. Because of the mechanical deformations, the *c* crystallographic axis of calcite is preferentially perpendicular to the plane of compression molding and the direction of stretching in a variety of polymer composites of low-density polyethylene, polypropylene, impact-resistant polystyrene, and plasticized poly(vinyl chloride) containing different additives.

Introduction

The electron paramagnetic resonance (EPR) method has been recently applied to the study of the orientation in the amorphous regions of polymers.[1-3] In this work paramagnetic molecules were introduced into the amorphous region of elongated polymer films and the order parameter of the partially oriented molecules was derived from the angular dependence of the EPR spectra.

We have also developed an EPR method in order to investigate the mechanically produced orientation of the fillers in polyethylene composites.[4] In this case the Mn^{2+} impurity centers and the trapped electrons in the filler served as natural "spin probes". The advantage of our method is that beside the experimental simplicity (no irradiation and sophisticated chemical treatment is required for introducing the probing additives and the samples can be investigated at room temperature) the investigated orientation effects characterize directly the interactions between the crystallites of the filler and the polymer chain, which plays a dominant role in the modifications of mechanic properties of the polymer composites.

In this paper the orientational properties of some industrial fillers (Durcal 2 and Millicarb; milled $CaCO_3$)[5] were studied and methods are developed for the complex characterization of the orientation produced by the compression molding and stretching of different polymer composites. The degree of orientation is compared for polyethylene (PE), polypropylene (PP), polystyrene (PS), and plasticized poly(vinyl chloride) (PVC) composites. The effect of an elastomer (EPDM) is also studied.

Experimental Section

Polymer Composites. The following compounds were used: PE, 80 wt % low-density polyethylene (Typolen: FA 2210, TVK, Hungary) and 20 wt % filler (Durcal 2, milled $CaCO_3$ with average particle diameter 3 μm, produced by Omya); PP/1, 80 wt % polypropylene (ethylene–propylene copolymer with an ethylene content less than 5%, TVK, Hungary; Typolen K 501) and 20 wt % filler (Durcal 2); PP/2, 70 wt % polypropylene (K 501),

0024-9297/85/2218-0918$01.50/0